2015

Surface photovoltage transients for p-type AlGaN

Karen L. Phumisithikul
Virginia Commonwealth University

Surface photovoltage transients for p-type AlGaN

A Thesis submitted in partial fulfillment of the requirements for the degree of
Master of Science in Physics and Applied Physics at Virginia Commonwealth University.

By:

Karen Lee-Ann Phumisithikul

Bachelor of Science in Physics and Applied Physics

Virginia Commonwealth University, 2013

Director:

DR. MICHAEL A. RESHCHIKOV

ASSOCIATE PROFESSOR, DEPARTMENT OF PHYSICS

Virginia Commonwealth University

Richmond, Virginia

May 4, 2015

Acknowledgments:

I am truly grateful and thankful to all those who have guided and supported me to this very moment in my life. This achievement couldn't have been done alone without the influences of several individuals, which I would like to express with sincere gratitude to all of them.

First of all, I want to express my deepest gratitude to the person who taught me how to be a better scientist and knowledgeable student in everything he knew in his field. I never would have experienced anywhere else without my adviser, Dr. Reshchikov. An inspirational lesson that you've taught me—and have even shown me through your personal experience in speeches, teachings, and marathons—is to "*Never give up!"* It is really inspirational for a professor I regard with the highest respect to share his experiences of how he became a better scientist. I was never an athletic one but I want to thank you for helping me get through my personal marathon.

Dr. Baski, I have never appreciated how simple things can be easily explained once you have mastered the concept much more than I do today. I truly appreciate the feedback you have given me to help me grow as a physicist. The experiences and the "3 item" speech that you have shared have encouraged me to be a more confident female scientist.

To my lab mates—Nahla and Joy—for creating a lab full of non-stop learning and self-improving with positive support! Nahla, I am thankful for the support and study sessions! Joy, thank you for answering the "quick questions" and helping me in so many ways that's beyond the lab and research! I wouldn't have grown as a student and person without the aid from you two.

Erick and David thank you for cheering me up and helping me not overthink the little things. Erick Robin Pope, you have shared so many hilariously insane stories that helped me stay sane! David, thank you for keeping everything in perspective and mellow!

Mum and Dad, I made it! I want to thank you for all you've done for me. I appreciate all the support and affection that you expressed through phone calls, emails, stories and delicious meals. Many thanks to my sister, Kathryn, for making life, especially graduate school life, much sweeter with the surplus of sweets and delicious goods you always send me when I need any.

Most importantly, the one who I turn to the most when I want to explain new topics numerous times or obtain positivity from is my best friend, Herbert. I appreciate you for all the little things you do and I am very grateful for the patience and affection you exponentially give.

To the VCU Physics Department thank you for all the wonderful fulfilling lessons and memories.

Table of Contents

List of Figures (captions):

Abstract:

Surface photovoltage transients for p-type AlGaN

By Karen Lee-Ann Phumisithikul

A Thesis submitted in partial fulfillment of the requirements for the degree of
Master of Science in Physics and Applied Physics at Virginia Commonwealth University.

Virginia Commonwealth University, 2015

Major Director:
Dr. Michael A. Reshchikov
Associate Professor, Department of Physics

There is an understanding of surface photovoltage (SPV) behavior for GaN, yet little is known about the SPV behavior for AlGaN. In this work, a Kelvin probe was used to measure the SPV for *p*-type AlGaN. Very slow SPV transients were found in AlGaN, which could not be explained with a simple thermionic model. A possible explanation of this behavior is the segregation of impurities to the surface, which causes significant reduction of the depletion region width (down to 2 nm), with carrier tunneling and hopping becoming the dominant mechanisms responsible for the SPV transients. To verify this assumption, the near-surface defective region (about 40 nm) has been removed through the ICP-RIE process. After the etching, the SPV transients became fast and increased in magnitude by about 0.6 eV. By using the thermionic model, band bending was estimated to be -1 eV.

Chapter 1. Introduction

AlGaN materials have the potential to contribute to higher efficiency devices and applications in a world where energy conservation is necessary. Solid-state lighting over the years has progressed and evolved such that countries all over the world use and need electrical light sources for daily life. With more people requiring electrical usage, researchers and companies are seeking light sources that are energy and cost efficient along with being sustainable.

LEDs (**Fig. 1-1**) have contributed to society since 1962 when they first came out on the market. [1] Laser diodes (LDs) and light emitting diodes (LEDs) have been ingrained into daily life, such as bar code reading, visual signals, Blu-ray players, illumination, fiber optic communication, and even as a surgical tool for hemostasis. GaN is a semiconductor that pushed the LED/LD forward because it was applicable to high power, high frequency devices due to its optoelectronic properties which allows it to make laser diodes in the UV (405 nm) region possible without frequency doubling.[2,3]

GaN is currently used as a high electron mobility transistor, LD, and LED. With such a wide application, it is imperative to find the next improved alternative. AlGaN/GaN heterojunctions are often used for High-electron-mobility transistors (HEMTs) due to the wider band gap and for UV LEDs, to push further into the UV spectrum (down to 205 nm). This makes AlGaN a very promising material for its unique properties for high energy. Therefore, in order to use AlGaN to its maximum potential, more properties of the material need to be understood.

1.1. Motivation

This work began as a collaborative effort with the College of Nanoscale Science and Engineering, SUNY Polytechnic Institute, Albany (Prof. F. Shahedipour-Sandvik). SUNY's main interest in AlGaN, especially *p*-type AlGaN, is related to the development of III-Nitride UV photocathodes which have been found to be highly sensitive to surface properties. From their photoemission experiments, they obtained controversial results and require additional

information on the surface band-bending in *p*-type AlGaN. There are no known studies on this subject. Knowing the surface band bending in these *p*-type AlGaN films will lead to improved performance of photocathode devices.

1.2. GaN material

GaN is currently a well-known material that has been used to produce bright white and blue LEDs. In the world of science and technology, scientists are trying to improve the materials that we currently have to produce a better material or product. Scientists are exploring different variations of III-nitride systems with GaN as their base foundation. GaN is a semiconductor commonly used for white and blue LEDs (**Fig. 1-3**). It is a hard compound with a wurtzite crystal structure (**Fig. 1-2**) and a wide band gap (3.43 eV at room temperature) which allows it to be used for optoelectronics, high power, and high frequency devices.[4] The material has a high heat and thermal capacity. It can be doped with Mg to produce *p*-type, or with Si to produce *n*-type. However, once doped, it adds additional tensile stress to the compound which makes it more brittle.

1.3. AlGaN material

AlGaN, which is an alloy of GaN and AlN, is not a very well-studied material. While the properties of bulk AlGaN and AlGaN quantum wells (**Fig. 1-4**) are better understood, there is almost no knowledge of the effect of the AlGaN surface on its electrical and optical properties. AlGaN has not been a well explored material in the scientific community, except for its use as a buffer in some materials.[5] Due to previous and plentiful studies of the optical and electric properties of GaN, there is some expectation and understanding of the material system, but these assumptions should be experimentally verified. In this work, four samples of AlGaN with various Al compositions (6-17%) were studied using a Kelvin probe. The surface potential behavior was observed and measured at different ambients (vacuum or air) or at different temperatures (300-500 K). AlGaN has a bandgap smaller than the photon energy of the HeCd laser (3.8 eV) used in our measurements.[6] Since there are no reports on the band bending and

SPV in AlGaN, typical methods of experiment that were used in the past for GaN samples were used to study the samples and an attempt was made to estimate the band bending.

1.4. Band bending in GaN

Band bending is the change of potentials at the surface of a semiconductor due to accumulation of charge at the surface. There are two types of band bending: upward and downward. In *n*-type GaN, negative charge at the surface causes the bands to bend upwards as they approach the surface. The origin of the negative charge at the surface is unknown, but most likely due to dangling bonds, impurities at the surface, or adsorbed species such as oxygen. The negative charge is compensated with the positive charges created by empty shallow donors in the depletion region. The width of the depletion region in *n*-type GaN is about 100 nm, and the exact value depends on the concentration of uncompensated shallow donors. The value of band bending is ~ 1.0 eV in *n*-type GaN.[7] Similarly, in *p*-type GaN, the bands bend downward at the surface due to positive charge at the surface. The values for band bending in *p*-type are disputed, and are estimated to be ~2eV downwards.[8]

1.5. Surface photovoltage

Surface photovoltage (SPV) is the change of the potentials (or in the value of the band bending) under light exposure. SPV measurements monitor the potential of a semiconductor surface under illumination. A laser with above-bandgap light (3.81 eV) is used to generate electron-hole pairs in the depletion region, which are then quickly separated by presence of a strong electric field. The photo-generated holes are swept to the surface in *n*-type (to the bulk for *p*-type) and the photo-generated electrons are swept to the bulk for *n-type* (to the surface for *p*-type).

Due to the electric fields at the surface, there exists a depletion region close to the surface where the carrier density is significantly reduced. The decrease in carrier density leads to band bending away from the Fermi level (due to a net charge at the surface) and creates a surface potential. If the material is exposed to above bandgap light, the minority carrier generated (either

a hole or electron – whichever is less abundant) drift towards the surface and as a result leads to more carrier density at the surface which leads to less band bending away from the Fermi level (becomes more neutral) . Therefore this leads to a change in the surface potential under illumination. Calculating the difference in surface potential is a method of estimating the band bending of the material.

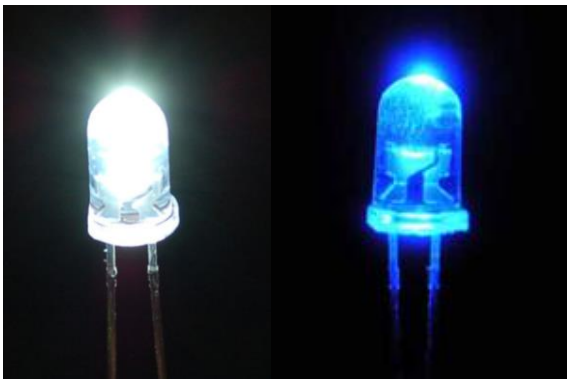

Figure 1–1. White (left)[9] and blue (right)[10] LEDs

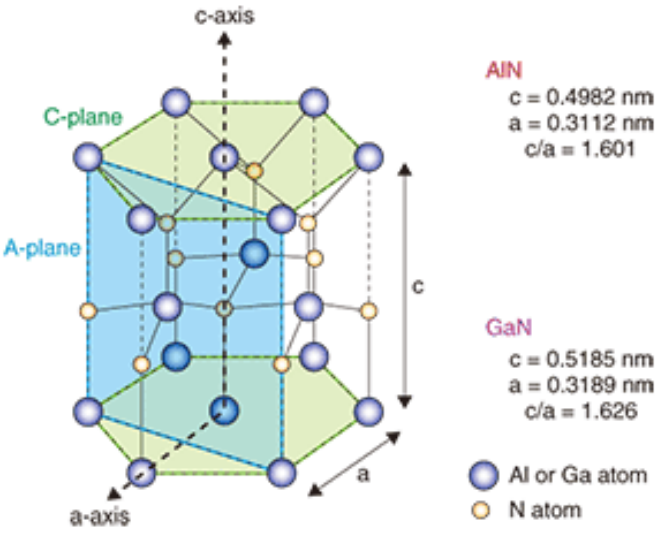

Figure 1–2. Al and GaN crystal structure.[11]

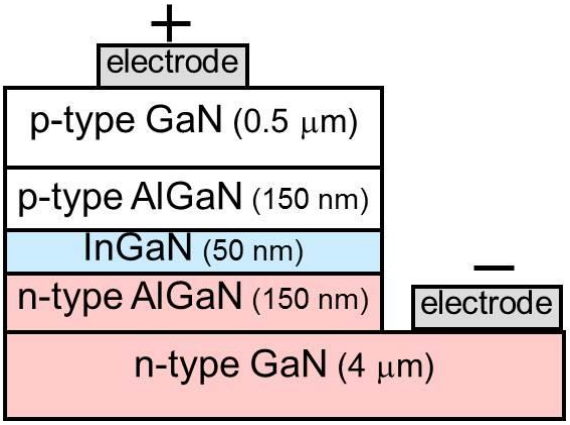

Figure 1–3. Schematic of a blue LED.[12]

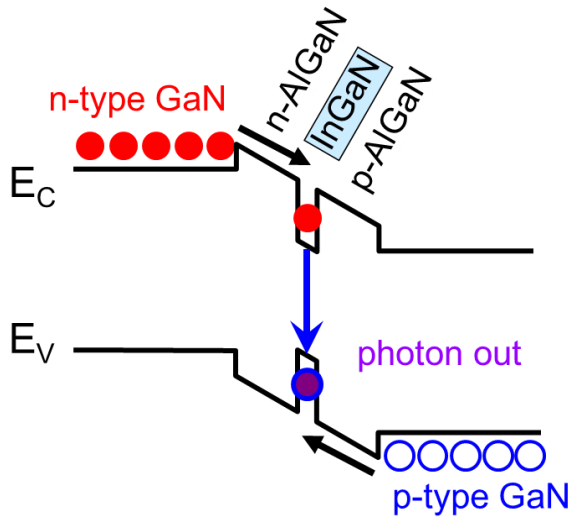

Figure 1–4. Quantum well formed by AlGaN/InGaN localizes electrons and holes in the same region for a more effective recombination to form photons.[13]

Chapter 2. Literature Review

2.1. Determination of the Al mole fraction and the band gap bowing of epitaxial $Al_xGa_{1-x}N$ films[4]

Angerer et al., made a variety of AlGaN samples with varying mole fraction compositions. They grew the AlGaN on sapphire using plasma induced molecular beam epitaxy at temperatures from 840 - 1000°C and determined the composition of Al to GaN using x-ray diffraction. AlGaN was found to follow Vegard's rule, a method to calculate the bandgap energy of a mixture by making the assumption that the two constituents mixed together will have the same crystal lattice so they will exhibit a weighted mean in their bandgap energies depending on their fraction in the mixture. In this case as the Al mole fraction increased from 0 - 1, the absorption coefficient/band gap increased from 3.45 eV to 6.15 eV with a bowing parameter of 1.13. (The bowing parameter is a measure how much the relationship deviates from Vegard's rule). For the samples used in our work which had varying Al compositions we estimate band gap values to be similar to the values as seen in **Figure 2-1** while using the above information.

2.2. Energy band bowing parameter in $Al_xGa_{1-x}N$ alloys[14]

Varying AlGaN compositions were prepared using molecular beam epitaxy on sapphire at 600 - 670°C and the band gap was analyzed. Using secondary ion mass spectrometry and Rutherford backscattering, the mole fraction composition was deduced from 0 - 1. The bowing parameter was found to be 1.0 eV. The bandgap increased as the Al composition of AlGaN was increased from 3.5 eV to 6.2 eV (mole fraction of 0 - 1 respectively).

2.3. Determination of Band-Gap Bowing for $Al_xGa_{1-x}N$ Alloys[15]

The authors in this work studied AlGaN grown on sapphire using MOCVD at 1000°C by using X-ray diffraction. They found that in many other papers there is a large range of the bowing parameter (-0.8 - +2.6 eV) and found that this may be due to complicating factors such

as strain and defects. Therefore it seems that simple X-ray diffraction cannot be used to deduce the composition in mole fraction. They used a thickness correction procedure to calibrate the X-ray diffraction. The correction factor was dependent on the varying thickness and strain. After correction, the bowing parameter of 1.38±0.01 eV was determined.

2.4. The band-gap bowing of $Al_xGa_{1-x}N$ alloys[16]

S.R. Lee and et al, made AlGaN with varying Al compositions from 0 to 0.45. They grew AlGaN on sapphire using metal organic chemical vapor deposition (MOCVD). However, unlike other studies, AlGaN was grown at differing temperatures that ranged from low to high temperature, which seemed to effect bowing parameters. At higher temperatures (>800°C) the bowing parameter, was >1.3 eV while at lower temperatures the bowing parameter was <1.3 eV.

Looking at these studies, we see that band gap is dependent on one major factor, and that is it follows Vegard's law. As the mole fraction of Al increased, the bandgap of AlGaN also increased. Furthermore there does seem to be a temperature dependence on the bowing parameter as shown by Lee, et al. Therefore, further analysis of AlGaN materials must be done in order to see the dependence of temperature and composition on the SPV and band bending.

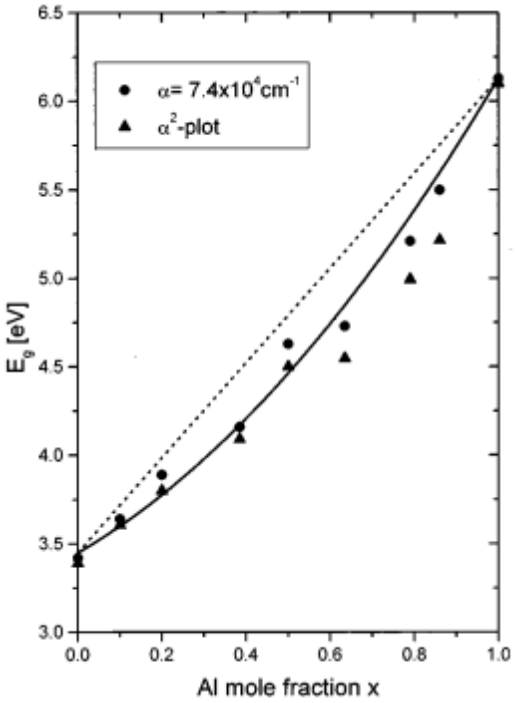

Figure 2–1. H. Angerer: Band gap of the $Al_xGa_{1-x}N$ films vs. Al content. The solid line was calculated Vegard's law and a bowing parameter of b = 1.3 eV. In addition to the energy gap determined at $\alpha = 7.4\times10^4 cm^{-1}$ (circles), E_g determined from the α^2 dependence on energy is also shown (triangles)

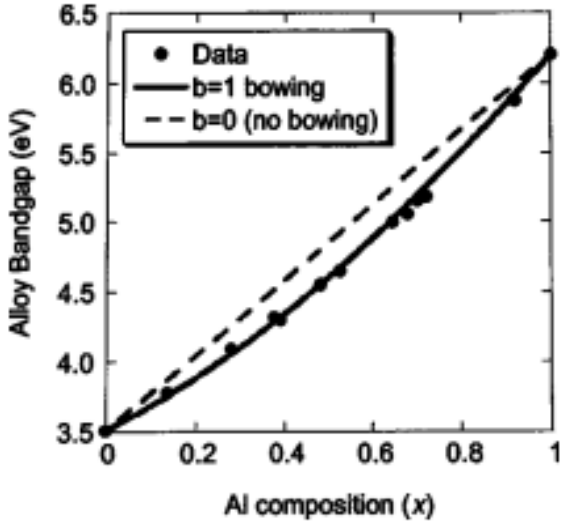

Figure 2–2. Feng Yun: Experimental data of energy band gap of AlGaN ($0\leq x\leq 1$) plotted as a function of Al composition (solid circle), and the least squares fit (solid line) giving a bowing parameter of b = 1.0 eV. The dashed line shows the case of zero bowing.

Chapter 3. Experimental Details

The main instrument used for this experimental process was a Kelvin probe setup (McAllister Technical Services, KP6500).[17] The instrument held samples that were exposed to different ambients and environments and differing set temperatures. The Kelvin probe allowed the data of the potential difference of two surfaces to be collected.

3.1. Kelvin Probe setup

The Kelvin Probe is used in this work to measure the charge at the surface and the SPV of the AlGaN samples. The Kelvin probe measures the potential difference between two surfaces. This instrument measured the potential difference between the sample and a vibrating probe which are arranged in a parallel plate capacitor arrangement. These measurements are all done horizontally in the *x*-axis direction where the probe is oscillating back and forth in respect to the sample surface. Refer to **Figure 3-1** for Kelvin Probe schematic. The behavior of the surface potential was measured when exposed to various temperatures, ambient and environments. Since the Kelvin probe is mounted inside of an optical cryostat (Janis Research Co.), low pressure can be achieved (~5×10^{-6} mbar) inside the chamber, or the chamber can be filled with air or oxygen. A sapphire window on the cryostat is used to allow the laser light to shine on the sample which is mounted inside the cryostat. Neutral density filters (i.e. 10^{-4}, 10^{-3}, 10^{-2}, and 10^{-1}) outside of the cryostat are used to attenuate the laser intensity, for intensity dependent measurements. The laser used in this work is a HeCd, continuous wave laser, with energy equal to 3.81 eV.

The theory for the Kelvin probe is based on the time-varying change in surface charges of the sample in respect to a metal probe. A potential is generated between the two surfaces (probe and sample) when they are brought into close contact. The probe measures the contact potential difference (CPD) of the sample which is simply the difference in work functions, and is the amount of energy required to release electrons from a surface. When these two different materials are brought close together and are connected by a wire, the work functions equalize

and electrons flow from the lower work function to the material with the higher work function making one material positive while the other is negatively charged. The difference in charges creates an electric potential. Once the materials' electric field compensates for their difference in work function, electron transfer stops. The electric potential necessary to equalize the work functions is defined as the contact potential difference (CPD). A voltage is developed between the materials and a backing potential is applied so that the charges are removed and once the charges return to neutral (can also be called the null point) the backing potential becomes equal to the CPD and this is the signal which is output by the Kelvin probe program.

In order to produce the measurement readings, the probe vibrates to produce a varying capacitance that is represented by the following expression

$$C = \frac{\varepsilon \varepsilon_0 A}{d}, \qquad \textbf{(3.3-1)}$$

where C is capacitance, A is the area of the parallel plate, and d is the separation distance between the plates.[17] The capacitance or the charge divided by the voltage is inversely proportional to the distance between the two materials. Therefore, as distance increases, capacitance decreases and since charge remains the same, the voltage must increase. As the probe oscillates, the voltage changes and can be fit using a sinusoidal function. The software will automatically calculate the null point from the sinusoidal function into a linear line which is then interpreted as the CPD.

The direction of the CPD signal under illumination can show the conductivity type of any given sample. For instance, a positive increase in the CPD signal (signifying a positive SPV) indicates *n*-type conductivity since the surface becomes less negative. For *p*-type conductivity, the CPD signal increases in the negative direction, as the surface becomes more negative. See **Figure 4-3** for expected SPV behaviors for GaN.

3.2. Aluminum Gallium Nitride samples

There were four *p*-type AlGaN samples that were researched in this work. These samples had variations of Al composition which ranged from 6% to 17% which we received from SUNY, Albany, New York. The AlGaN samples were grown through a process called metal organic chemical vapor deposition (MOCVD) and then doped with magnesium (Mg). The Al composition of the AlGaN was varied by changing the TMAl (trimethlylaluminum) flow in set increments (i.e. 5 standard cubic centimeters at a time). The growers didn't have information about how the composition of the *p*-type AlGaN would change under gas flows which is why the composition values vary arbitrarily. See **Table 3-1** for a list of additional detailed information of the AlGaN sample specifications. Overall, the top layers of the samples range from 270 – 315 nm (see **Figure 3-1** which shows the sample thickness and layer types) on top of a layer that is 80% of undoped AlGaN (~500nm), AlN (~10 μm), and Sapphire (0.4 mm). The undoped AlGaN layer between the *p*-type AlGaN (top layer) and AlN is unknown in comparison to the top *p*-type AlGaN which is known.

3.3. Experimental Procedures

Since these samples were expected to have similar behavior to *p*-type GaN samples, similar methods to previous *p*-type GaN measurements were performed. [12, 13] Specifically, the extremes of Al compositions (6% and 17%) were first tested to get a general idea of the behaviors that could be seen between the composition differences. The samples were first exposed to UV in air ambient and the SPV was measured. Then, the SPV was measured as the samples were exposed to UV in vacuum. Various heat treatments were used following a published method of achieving faster band bending restoration by heat treatment.[8] Room temperature measurements were also performed after heat treatments, to observe any irreversible changes in SPV behavior due to the annealing.

Before any SPV measurements were taken on the samples, they were all kept in dark at room temperature for at least one to two days. Overall, measurements were usually taken in

chronological order such as the following sequence: RT – air and vacuum; annealing; cooling then, RT – vacuum and air. All samples usually began with SPV measurements in air at room temperature exposed to 1 hour of UV. Next, SPV measurements were taken in vacuum exposed to 1 hour of UV at room temperature then various temperatures (400K, 500K, and 600K). Afterwards, SPV measurements were taken in vacuum at room temperature exposed to 1 hour of UV after annealing at various temperatures. Two samples (6% and 17% Al) were exposed to oxygen gas for additional measurements. Since the experimental results of all the samples were not showing typical well-modeled behaviors of *p*-type behaviors, we devised a theory which involved etching the top 40 nm of the samples.

The etching process that was used during this experimental procedure to remove the impurities in two of the four samples (6% and 17%) was the inductively coupled plasma (ICP) reactive ion etching (RIE) method. With the given information of our *p*-type samples being 280nm and 315 nm for the 6% and the 17% Al composition, respectively, we determined that 40 nm would be a proper amount to etch off the top layer. Before the etching process began, the four metal contacts on our samples were protected by photoresist paint. The machine used to etch in ICP-RIE process was a SAMCO RIE-101 iPH.

3.4. Experimental Procedures after Etching

The two samples chosen to be etched were the extreme concentrations of Al composition which were 6% Al (g3129ap) and 17% Al (g3193ap). The procedures for these samples included, first, 1 hour SPV measurements in air and vacuum at room temperature. Second, intensity dependence was measured in air and vacuum at room temperature, by using neutral density filters to change the intensity of the laser. The time of UV exposure depended on the time for the SPV signal to saturate, which meant that the time duration was arbitrary. Then, these samples were measured for intensity dependence in vacuum at 500K. The room temperature intensity dependent measurements were again repeated after heating to 500K to see if the annealing had any effect on the SPV behavior.

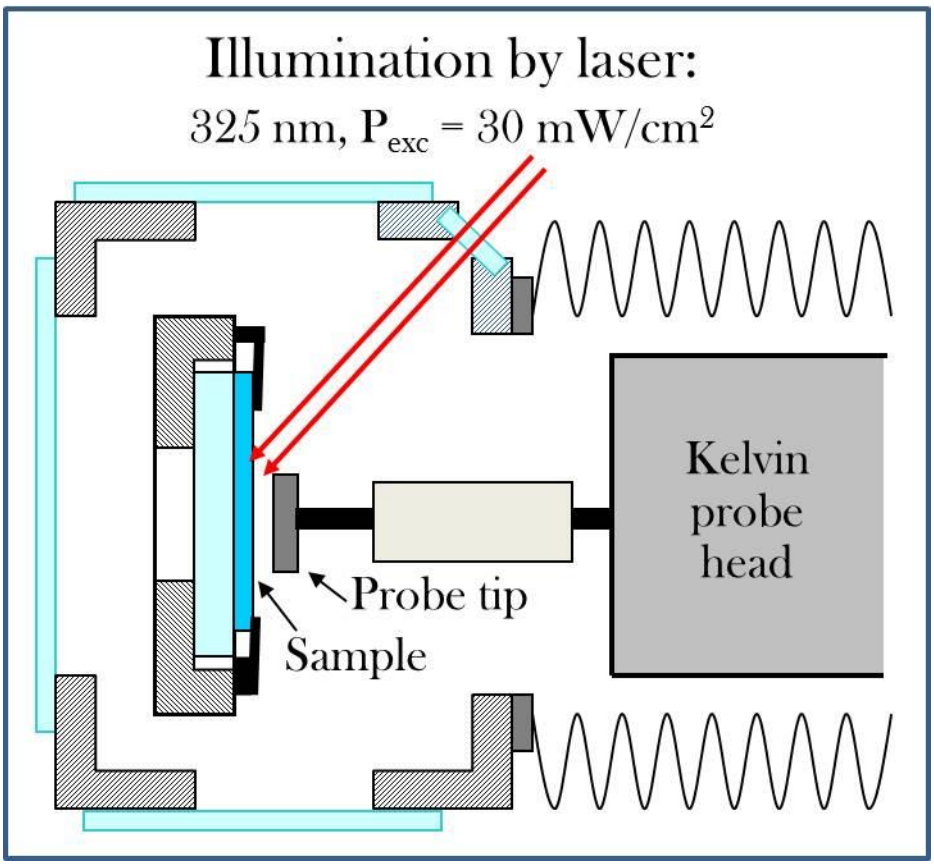

Figure 3–1. Schematic of the Kelvin probe from the top view of the cryostat.

Sample	Al %	Top pAlGaN layer thickness	Mobility $[cm^2/Vs]$	Carrier Conc. $[cm^{-3}]$
g3129ap	6	280 nm	5.15	1.08E17
g3192ap	9	270 nm	3.22	1.11E17
g3133ap	14	310 nm	0.819	7.96E17
g3193ap	17	315 nm	2.47	6.55E17

Table 3-1. AlGaN sample specifications.

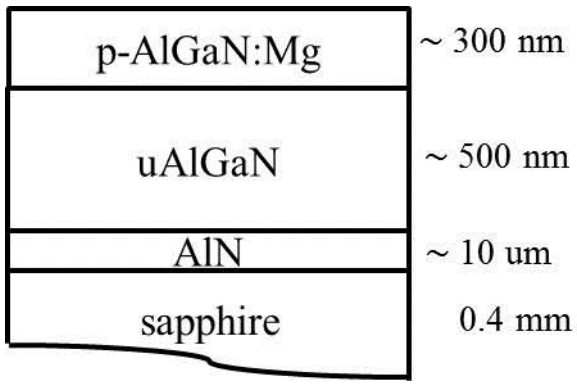

Figure 3–2. Schematic of AlGaN sample layer thickness and layer type.

Chapter 4. Theory of Surface Photovoltage in *p*-type AlGaN

4.1. Modeling of Band Bending in GaN

Surface band bending expected for GaN and its alloys is shown in **Figure 4-1** for both *n*-type and *p*-type. Let us for simplicity consider the band bending near the surface of *p*-type GaN (**Figure 4-1a**). The conduction band at the top of the diagram is labeled E_C and is followed by the dotted Fermi level, E_F which is near the valence band, labeled E_V. GaN has a band gap E_g = 3.4 eV in the bulk section. The band bending region between the surface and bulk is called the depletion region, having width *W*. The width of the depletion region *W* ~10 nm for the concentration of uncompensated acceptors on the order of 10^{19} cm^{-3} (for *n*-type it is about 100 nm for the concentration of free electrons on the order of 10^{17} cm^{-3}). The difference in the surface potential U_s and bulk potential U_b is band bending in dark that is denoted as Φ_0. The charge at the surface can be influenced by absorbed species, or dangling bonds. Oxidation may also occur at the surface.

4.2. Modeling Surface Photovoltage behavior

The magnitude of band bending for *p*-type (and *n*-type) in dark will decrease upon illumination with a UV laser (**Figure 4-2**). Electron-hole ($e^- - h^+$) pairs are created in the depletion region then immediately separated due to the electric field in the region. For *p*-type, the holes move into the bulk and electrons (negative charge) move to the surface causing the total positive *p* charge at the surface and the magnitude of the downward band bending to decrease. As for *n*-type, electrons move into the bulk and holes (positive charge) move to the surface causing the total negative *n* charge at the surface to decrease as the well as the upward band bending. The surface photovoltage (SPV) is defined as the difference between the band bending in dark, Φ_0, and the new band bending in light, Φ_{Light}, which can be denoted as *y*.

4.3. Graphing Surface photovoltage behavior in time

The general *n*-type and *p*-type SPV behavior can be seen in **Figure 4-3**. For a typical *n*-type sample, we have the change in CPD (eV) equal to the SPV along the y-axis and time (sec) is plotted along the *x*-axis (**Figure 4-3b**). We let the sample stay in dark to record a reliable baseline. Then, we expose the sample to UV for a certain amount of time depending on the experiment. For *n*-type, when exposed to UV, the SPV jumps upward and gradually increases until the signal saturates and reaches a constant value. Once the UV is turned off we have a restoration of the SPV in dark. The restoration can be fit with a logarithmic in time dependence based on the simple thermionic model of charge carriers in the presence of band bending.

4.4. Thermionic Model

The thermionic model is based on the assumption that there is Boltzmann distribution of free electrons by energy in the conduction band (in *n*-type semiconductor) or free holes in the valence band (in *p*-type). The electrons that have enough energy to pass over the barrier (upward band bending) in *n*-type can reach the surface and be trapped at surface states. Similarly, free holes in *p*-type semiconductor may have enough thermal energy to overcome the near-surface barrier for them (the downward band bending) and be trapped by the surface states. The transitions of the charge carriers from bulk to the surface and back obey Boltzmann statistics. Other mechanisms of charge transfer, such as tunneling and hopping, are ignored in the thermionic model. According to the thermionic model, the restoration of the SPV of the sample after illumination once the sample is in dark occurs due to electrons in *n*-type (holes in *p*-type) overcoming the near surface barrier and restoring the charge corresponding to the equilibrium (dark) conditions. The thermionic model is used to fit the SPV restoration dependences to show if the band bending restores according to the thermionic model.

For *p*-type, an expression for the decay of SPV as a function of time is derived from the thermionic model shown as,

$$y(t) \approx y_0 + \eta kT\left(1+\frac{t}{\tau}\right), \qquad \textbf{(4-1)}$$

where y_0 is the SPV after illumination has ended, η is the ideality factor, k is Boltzmann's constant, t is the time when UV illumination is switched off, and τ is the time-delay constant that has an exponential dependence on the band bending value instantly after illumination.[7] The key parameters that indicate that if the measurements fit our model is the ideality factor η which must be 1 in the thermionic model and the time-delay constant τ that is much less than 1 s for typical parameters of *n*- and *p*-type GaN.

4.5. Band-bending Model

To determine the band bending in *p*-type AlGaN, the SPV data must be fitted with the thermionic model.[7] The following equations were used for the steady-state SPV signal (in saturation):

$$y_0 = \eta kT \ln\left(1+\frac{cP_0}{R_0}\right) \qquad \textbf{(4-2)}$$

with

$$R_0 = s_p N_V \exp\left(\frac{\Phi_0 + (E_V - F)}{\eta kT}\right), \qquad \textbf{(4-3)}$$

where R_0 represents the rate of the holes overcoming the barrier near the surface and moving from the bulk to the surface; s_p represents the surface recombination velocity for holes (*p)*; N_V represents the effective density of states in the valence band; Φ_0 is the band bending in dark; $(F - E_V)$ represents the energy distance from the Fermi level to the top of the valence band; η is the ideality factor expected to be 1 in the thermionic model; k is Boltzmann's constant; and T is temperature. By combining **Eqns. (4.2)** and **(4.3)**, the SPV value can be derived to be

$$y_0 \approx \Phi_0 - (F - E_V) + \eta kT \ln\left(1 + \frac{s_p N_V}{cP_0}\right), \qquad \textbf{(4-4)}$$

where c represents the geometric factor that is a fraction of photons absorbed in the depletion region and P_0 represents the excitation intensity.[7] The R_0 values can be obtained from the fit of dependences of SPV on the UV light intensity, and then the band bending can be determined from **Eq. (4.4).**

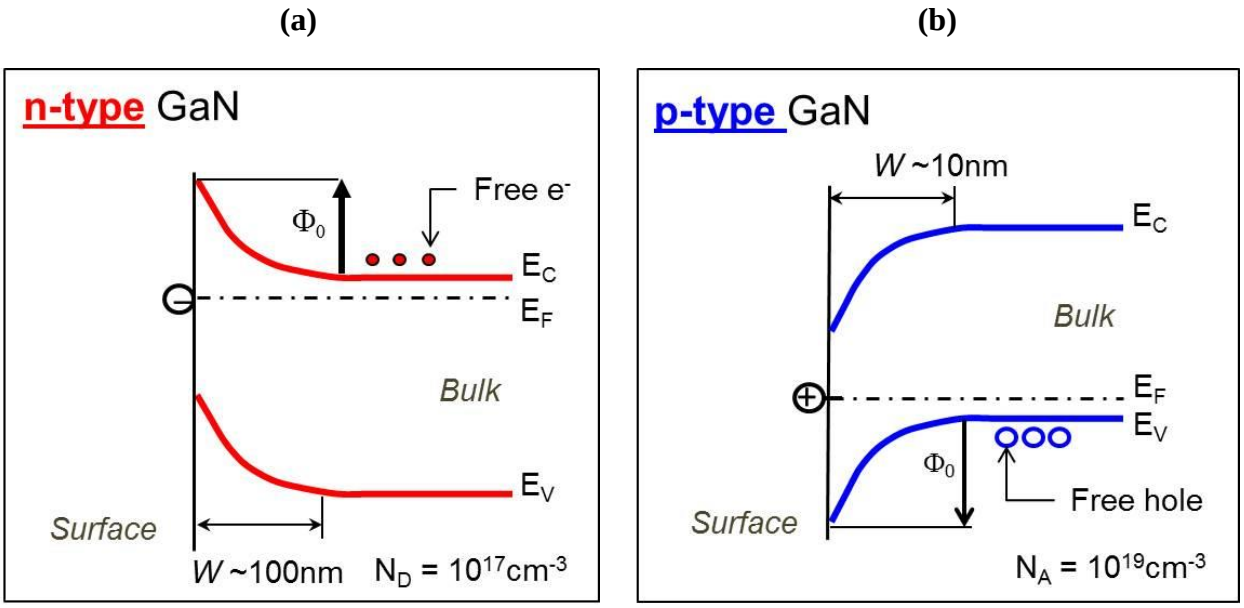

Figure 4–1. Surface band bending in **(a)** *n*-type and **(b)** *p*-type GaN.

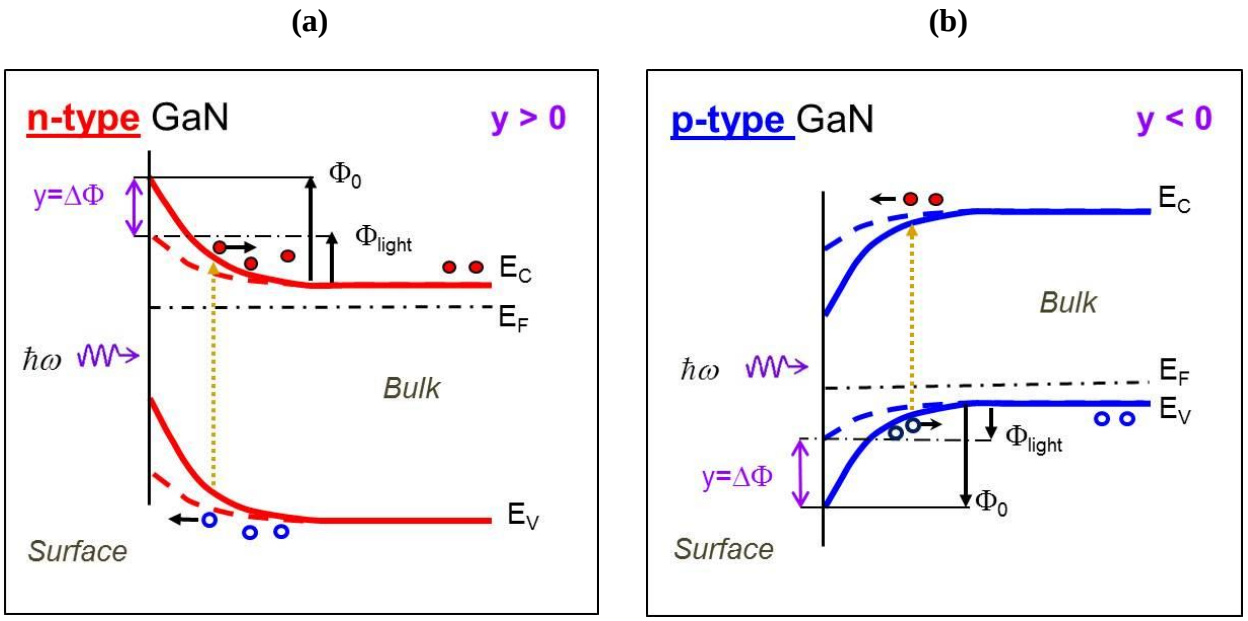

Figure 4–2. Surface photovoltage in **(a)** *n*-type and **(b)** *p*-type GaN.

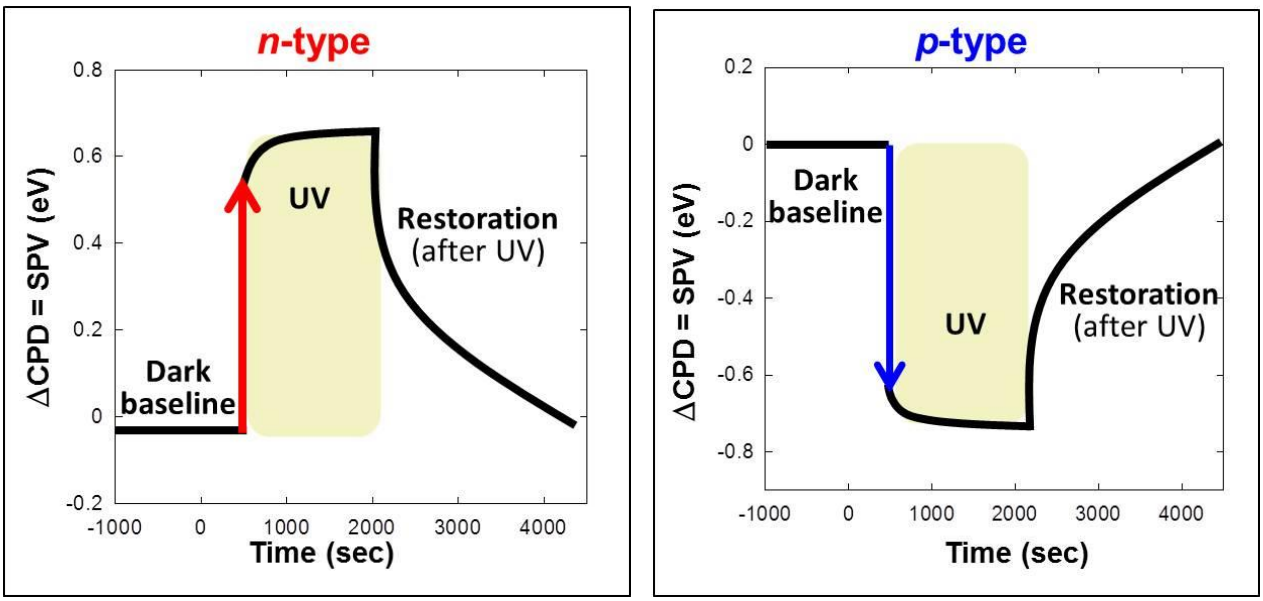

Figure 4–3. Expected *n*- and *p*-type SPV behavior.

Chapter 5. Research and Analysis

5.1. SPV from as received AlGaN

All four AlGaN samples with different Al compositions were measured in different ambient (air or vacuum) and for various temperatures. Of the four AlGaN samples, two samples with extreme compositions of Al (6 and 17%) were studied in more detail for temperature dependence and the figures can be found in the appendix.

Experiments that were in air ambient and vacuum were repeated several times as needed before heating the samples, since in past studies on GaN, we observed that although heating reduced the time necessary for restoration, it sometimes has an irreversible effect on the SPV behavior. The measurements for all the samples at room temperature in air do not show any clear correlation between the SPV behavior and the Al composition in AlGaN (**Fig. 5-1**). Although, it can be seen that the SPV has a higher negative value, due to photo-adsorption of oxygen molecules (negatively charged) in comparison to vacuum measurements.

The measurements for all the samples at room temperature in vacuum also showed no clear trend in the SPV as the composition concentration increased (**Fig. 5-2**). The negative SPV values slightly increase upward, apparently due to photo-desorption of oxygen molecules (negatively charged) or any other charged molecules in vacuum. In comparison to air, the samples with 14% and 17% Al composition have smaller magnitudes in the downward SPV than the samples with Al composition of 6% and 9%.

The first important conclusion from the SPV transients (both in air and vacuum) is that the SPV signal becomes more negative under illumination, which confirms that all the AlGaN samples are indeed *p*-type, as was predicted from the growth conditions. The second and more important observation is that the SPV transients in air and vacuum at room temperature are very slow and the SPV values (at least in vacuum) are not restoring to their original baseline in any reasonable time (i.e., within a day or week). This is different from what we observed for GaN. To quicken the restoration process for the samples, annealing was done. Annealing at elevated

temperatures provides thermal energy to electrons (or holes) to overcome the potential barrier of the conduction band (or valence band).

5.2. SPV after Annealing

The SPV transients were measured at the temperature of the annealing and at room temperature after annealing in vacuum. **Figure 5-3** shows the SPV transients in vacuum at room temperature after preheating (annealing) at 500 and 600 K. We can see that there are ambiguous SPV behaviors that are not comparable to measurements in air (**Fig. 5-1**) or in vacuum (**Fig. 5-2**) nor are they comparable to results for *p*-type GaN.[18] **Figure 5-3** shows that the annealing process did not quicken the restoration process as it was observed previously for *p*-type samples[8], and that there were no fast transients as predicted by the thermionic model. It only appears that there are still slow transients. Furthermore, the delay time, τ , for the restoration to begin is significantly longer, indicating a secondary process which may be hindering the restoration of the band bending in the dark. According to the thermionic model, for light intensities used in this experiment, the change of the SPV upon illumination must be instantaneous (faster than one second, the temporal resolution for the Kelvin probe setup used in this experiment). On the other hand, after switching off the illumination, the logarithmic decrease of the SPV signal should begin at the characteristic time delay τ much smaller than one second (τ ~1s). However, in this experiment (**Figs. 5-1 to 5-3**), both transients are very slow; the initial SPV change upon illumination is very small and apparently logarithmic in time, while the restoration begins after a significant amount of time (longer than 1s).

A potential explanation for these slow transients in AlGaN can be related to the samples chemical property of being an alloy that can form an insulation layer very close to the surface, which slows the transfer of charge carriers over the barrier (the process of restoration). Another explanation for this slow transient is the segregation of defects and impurities to the surface, which affects the depletion region width and ability of charge carriers to reach the surface.

The following information is to explain the figure data in more detail. **Figure 5-1a** shows the time dependence of SPV in air ambient at room temperature. The UV light from the HeCd laser was switched on at time $t = 0$ and was switched off after about one hour. It can be seen that the SPV is negative and the absolute value of the SPV increases relatively slowly at $t > 0$. The SPV slowly changes as compared to typical transients observed for *p*-type GaN and is in disagreement with the thermionic model. In more detail, the initial change of the SPV at $t > 0$ can be seen in **Figure 5-1b**. From this figure, it can be seen that the SPV signal changes logarithmically with time, and the expected fast component of the SPV (expected to be much faster than one second) is apparently missing.

As **Figure 5-1a** shows, as the Al composition increases, the SPV magnitude increases. This may be due to the fact that the samples become more reactive when exposed to air ambient, and negative surface charge is expected to increase by the photo-adsorption of O_2 molecules on the surface of the samples.[18] **Figure 5-1b** shows the time dependence of the initial SPV in logarithmic scale. The UV light from the HeCd laser was turned on at time $t = 0$ s. It can be seen that the SPV magnitude increases very slowly at $t > 0$. Note that for the 6% Al measurement there was a break in the data at $t = 100$ to t = 400 s since the Kelvin probe was not able to acquire data during this time due to unknown equipment error.

Figure 5-1c shows the time dependence of the SPV restoration in logarithmic scale. It can be seen that the magnitude of the SPV starts changing only at $t = 10$ - 1000 s after the light was switched off. Overall, there are very slow transients in the restoration. This shows that there is a disagreement of the observed behavior with the thermionic model.

Figure 5-2a shows the time dependence of SPV in vacuum ambient at room temperature. The UV light from the HeCd laser was switched on at time $t = 0$ s, and was switched off after about one hour. It can be seen that the SPV is negative and the absolute value of the SPV increases relatively slowly at $t > 0$. The SPV changes slowly at $t > 0$ as compared to the transients in the *p*-type GaN and in disagreement with the thermionic model. In more detail, the initial change of the SPV at $t > 0$ can be seen in **Figure 5-2b.**

The SPV transients in a vacuum environment do not show any correlation from the Al composition. The SPV data taken in vacuum have ~0.3 eV increase in the range of all the samples (-0.2 to -0.5 eV) in comparison to the data taken in air (-0.58 to -0.88 eV). Another difference between SPV transients in vacuum and air is that the compositions 14% and 17% shift from the bottom of the SPV data in air to the top SPV data in vacuum. The shift increase in SPV can be caused by the photo-desorption of negatively charged surface species called photo-induced desorption, which decreases the amount of negative surface charges.

Figure 5-2b shows the time dependence of the initial SPV in logarithmic scale. The UV light from the HeCd laser was turned on at time $t = 0$ as shown in the logarithmic scale. It can be seen that the SPV transients are very slow at $t > 0$. It can be seen that for the 14% Al measurement the SPV logarithmic rate is the slowest at $t \approx 100$ – t ≈ 1000s in comparison to the other Al compositions. The initial SPV in logarithmic time dependence (**Fig. 5-2b**) has a steeper SPV slope than the data in air with the exception of 14% Al. Again, this can also be explained by photo-induced desorption of negative species on the surface.

Figure 5-2c shows the time dependence of the SPV restoration in logarithmic scale. At $t \approx 1000$ s the SPV only begins changing which shows that restoration is very slow when UV was turned off at time $t = 0$. This shows that there are slow transients that do not agree thermionic in vacuum ambient. These results are very similar to the restoration SPV behavior in air ambient at room temperature that can be seen in **Figure 5-1c**, but the time delay is much longer.

Figure 5-3a shows the time dependence of SPV in vacuum at room temperature after preheating exposure. These samples were preheated from one hour to 12 hours. The 17% Al sample was preheated at 600K whereas the other samples were preheated at 500K. The UV light from the HeCd laser was turned on at time $t = 0$ and, was switched off after about one hour except for the 17% Al sample which was switched off at $t \approx 2800$ s. It can be seen that the SPV is negative and the absolute value of the SPV increases relatively slowly at $t > 0$. The SPV changes slowly at $t > 0$ as compared to the transients in the *p*-type GaN and in disagreement with

the thermionic model. In more detail, the initial change of the SPV at $t > 0$ can be seen in **Figure 5-3b.**

Again there is no correlation on the SPV behavior with increasing Al composition for the samples at room temperature in vacuum after being exposed to heat. The SPV data range of the samples in vacuum after preheating has an expanded range (from -0.2 to -0.88 eV) in comparison to the data in vacuum before heating (from -0.2 to -0.5 eV). We expect that charge carriers (holes for *p*-type) are given thermal energy to overcome potential barriers and reach the surface when exposed to high temperatures in dark conditions. [8] This allows the restoration of the SPV signal and its return to the original baseline. Note that the 6% Al and 9% Al data switched positions in comparison to vacuum before heating.

Figure 5-3b shows the time dependence of the initial SPV in logarithmic scale. The UV light from the HeCd laser was switched on at time $t = 0$. Horizontal bars near the left vertical axis indicate the value of the SPV just before switching on the laser. It can be seen that the slope of the initial SPV transients is less steep in comparison to vacuum before heating.

Figure 5-3c shows the time dependence of restoration of the SPV in logarithmic scale. The UV light from the HeCd laser was switched off after one hour of exposure, and the restoration in the graph begins at time $t \approx 0$ s. Horizontal bars near the left vertical axis indicate the SPV value right after switching off the laser. The restoration of the SPV does not begin immediately, as predicted by the model. The delay before restoration is longer for the measurements taken after annealing than for the measurements taken before annealing. It appears that heating the samples at high temperatures made some permanent changes close to the surface which prevents the restoration of the SPV to its original baseline.

5.3. Accounting for Defect Segregation

A potential explanation for SPV transients not agreeing with the thermionic model and being very slow is the segregation of impurities to the surface of the samples, an effect which becomes more pronounced after heating at high temperatures. As schematically shown in **Figure**

5-4a, an ideal sample of *p*-type GaN or AlGaN with low composition of Al has a bulk concentration of acceptors (Mg impurity) on the order of 10^{19} cm^{-3}. As a result, the depletion region width is about W = 10 nm. When the UV laser illuminates the sample's surface, it generates electron-hole pairs which quickly separate due to the strong electric field in the depletion region.

We assume that due to segregation of Mg and other impurities and defects, the concentration of uncompensated acceptors may increase by 1 – 2 orders of magnitude near the surface. Then, the depletion region width will decrease down to about 2 nm, while the barrier height may remain about 1 eV (**Fig. 5-4b**). With such a thin barrier, holes may tunnel from the bulk region to the surface. Then, the thermionic model cannot be applied. Moreover, for such high concentrations of defects in the near-surface layer, the hopping of charge carriers may become very efficient because the distances between defects become very small. [19,20,21] The hopping will also cause non-thermionic behaviors, and can qualitatively explain the slow SPV transients. Indeed, trapping and de-trapping in the hopping transfer may be slow and weakly dependent on temperature. Finally, the non-monotonic changes in the SPV transients with variation of Al composition can be understood within this model. The SPV transients are mostly governed by the extent of defect segregation in any given sample, which may have no or little correlation with the Al composition in AlGaN.

There are three types of charge transfer in this model: tunneling, hopping and trapping. For tunneling when the depletion region is thin enough (1 – 2 nm), the holes are able to tunnel through the depletion region to the surface. For the hopping mechanism, holes are able to hop through defects to the surface from the bulk and the depletion region, but sometimes the electrons/holes will get trapped in the depletion region. Lastly, the other type of mechanism is the trapping of electrons/holes at defect states in the depletion region.

5.4. SPV from AlGaN after Etching

The assumption that the slow SPV transients are caused by a high concentration of defects and impurities near the surface due to their segregation from high temperature treatment can be verified experimentally. For this, we decided to remove the near-surface layer by etching and repeating the SPV measurements. The process of removing the defective layer was done by inductively coupled plasma reactive ion etching (ICP-RIE). From the four AlGaN samples, two samples with extreme Al composition (Al 6% and Al 17%) were chosen for this etching process experiment. According to the specifications of growers at SUNY, Al compositions are relevant to the top layers of 218 nm and 315 nm (Al 6% and Al 17%). From the surface of these top layers 40 nm was etched. As a result, significant changes in the SPV transients occurred. For both samples the SPV signal was significantly larger, and the restoration of the SPV began much faster, in better agreement with the thermionic model

Figure 5-5 shows the time dependence of SPV in air and vacuum ambient at room temperature for 6% Al after etching. The UV light from the HeCd laser was turned on at time t = 0 and switched off at $t \approx 1000$ s (in vacuum) and at $t \approx 3600$ s (in air). The SPV signal is negative and the absolute value of the SPV increases relatively quickly at $t > 0$ in comparison with the SPV transients before the etching. The negative SPV indicates the samples are still *p*-type after etching, in agreement with data taken before etching. The SPV changes quickly at $t > 0$, very similar to previously obtained SPV transients for *p*-type GaN and in agreement with the thermionic model. In more detail, the initial change of the SPV at $t > 0$ can be seen in **Figure 5-6**.

Figure 5-5a and **Figure 5-5b** show that the SPV data in air has a higher negative SPV magnitude, which may be due to the photo-adsorption of O_2 molecules and other negative species at the surface. Note that some data points are missing at $t \approx 0$ when the UV was turned on and near $t \approx 3600$ s (or $t \approx 1000$ s) when the UV light was turned off (see **Fig. 5-6**). The signal tracking at these time periods stopped due to the Kelvin probe not being able to record data

during that time. This is possibly because of the Kelvin probe adjusting to the current that was received from the full laser intensity.

From **Figure 5-5b** it can be seen that in air, the restoration to the baseline has been reached during the time of the experiment, except for in vacuum where the restoration still was not at full baseline. However, the time of restoration for both air and vacuum measurements is much shorter than the time required for restoration before the etching was performed. For both samples (6% and 17%), there are higher negative SPV magnitude values in air (-1.6 and -1.4 eV) than in vacuum (-0.8 and -1 eV), which may be due to photo-induced adsorption and desorption of negatively charged species in air and vacuum ambients, respectively. Remarkably, the SPV transients are much faster than in the experiments before the etching.

Figure 5-7a shows the restoration of SPV as the logarithmic in time dependence for the AlGaN sample with 6% Al in air and vacuum at room temperature. When the UV light from the HeCd laser is switch off at $t \approx 3600$ s (shifted to $t = 0$ for the logarithmic scale), the sample is left in dark conditions to restore to its original baseline. During restoration, the band bending of the sample is restoring to its original value in dark.

The thermionic model was used to fit the SPV restoration (shown with solid lines in **Fig. 5-7**). According to this model, the expected parameters are $\eta = 1$ and $\tau \ll 1$ s. Through Eq. (**4.4**), the values of R_0 and band bending can be determined. For the sample with 6% Al, the thermionic fits were calculated for air and vacuum using **Eq. (4-1)** with (**a**) y_0 = -1.58 and -0.78 eV; η = 3.3 and 3.1, $\tau = 4\times10^{-4}$ and 4.2×10^{-1} s; (**b**) y_0 = -1.45 and -0.52 eV; η = 3.38 and 2.65, $\tau = 6\times10^{-4}$ and 1×10^{-1} s.

5.5. Dependence of SPV on light intensity

During experiments for the etched AlGaN samples (6% and 17%), some data points are missing due to the Kelvin probe not being able to track any data when exposed to full intensity. As shown in **Figures 5-5** to **5-7** data points were missing up to $t \approx 20$ and $t \approx 300$ s. It is possible that this happened due to an overload in the current in the system which caused

overcompensation by the Kelvin probe and delayed measurement acquisition. To obtain the data points that were not measured at full laser intensity, various neutral density filters (with transparency from 10^{-10} to 10^{-1}) were used. In repeated experiments, it was found that narrowing combination of filters to (10^{-4} to 10^{-1}) was a better selection of interest for the data. As the laser intensity increased, the slope of the initial SPV transients decreased: for 295 K, the measurements had a linear decrease, whereas for 500 K, the SPV had a delayed linear decrease after 10^{13} - 10^{14} $cm^{-2}s^{-1}$. The SPV measurements required less UV exposure time to achieve SPV saturation.

These intensity dependences were measured in different environments and temperatures which allowed us to find the parameters of the thermionic model through fitting. With these parameters the band bending was calculated for the AlGaN samples (6% and 17%) at 500K whereas the band bending at room temperature (before and after the preheating) was estimated with much less accuracy because the SPV transients at room temperature could not be fit well with the ideality factor, η, close to 1. Intensity dependent measurements were taken for AlGaN samples with 6% and 17% (**Figure 5-8**).There are two measurements in vacuum at room temperature and one at 500K for sample with 17% of Al and two measurements for each temperature for the sample with 6% of Al.

5.6. Calculating the band bending in *p*-type AlGaN

From the intensity measurements collected from the two samples (6% and 17%) the R_0 values can be found by fitting the dependence with **Eq. (4-2)** and then the band bending can be calculated from **Eq. (4-3)**. Alternatively, the band bending can be found in one step as a fitting parameter in **Eq. (4-4)**. The effective density of states in the valence band N_V, for *p*-type, can be calculated with the following equation

$$N_V = 2\left[\frac{2\pi m_p kT}{(2\pi\hbar)^2}\right]^{\frac{3}{2}}, \qquad \textbf{(5-1)}$$

where m_p is the mass of a hole that is multiplied with the effective mass constant for GaN and $\hbar$ is Planck's constant.

We assume that the Fermi level is located at the same energy as the shallow Mg acceptor level. In GaN, the ionization energy of the Mg_{Ga} acceptor is 0.2 eV. In AlGaN with Al composition between 6 and 17%, the ionization energy of the Mg acceptor is expected to be slightly larger. We assume that $F - E_V = 0.25\,\text{eV}$ in these samples. The surface recombination velocity may vary in a wide range from sample to sample. Specifically, we can take a reasonable value of $s_n = 10^5 cm/s$, with the understanding that it may be off by an order of magnitude in one or another direction. The value of the geometric factor *c* may also have significant uncertainty. In GaN, the absorption coefficient is about $10^5 cm^{-1}$ at photon energy of the HeCd laser (3.81 eV). Then, in the depletion region where *W* = 10 nm, about 10% of the incident light will be absorbed, or $c = 0.1$. However, with increasing Al composition, the absorption coefficient at 3.81 eV will decrease. In addition, the concentration of uncompensated acceptors may be higher than previously mentioned due to defect segregation, about $10^{19} cm^{-3}$. As a result, the value of *c* may decrease by about an order of magnitude, down to 0.01.

These parameters enabled the calculation of the band bending to be about -2 eV at 295 K and about -0.9 eV at 500 K. The value of band bending at *T* = 500 K should be considered more

reliable because in this fit, the ideality factor η was 1. The value of band bending for the room temperature is questionable because the ideality factor η was much different from 1, and the application of the thermionic model for quantitative estimates in this case is doubtful. Note that in the first approximation, the band bending in dark should be independent of temperature (if the temperature-related shift of the Fermi level in bulk can be ignored). Thus, we conclude that in the studied *p*-type AlGaN samples the downward band bending is about -1 eV.

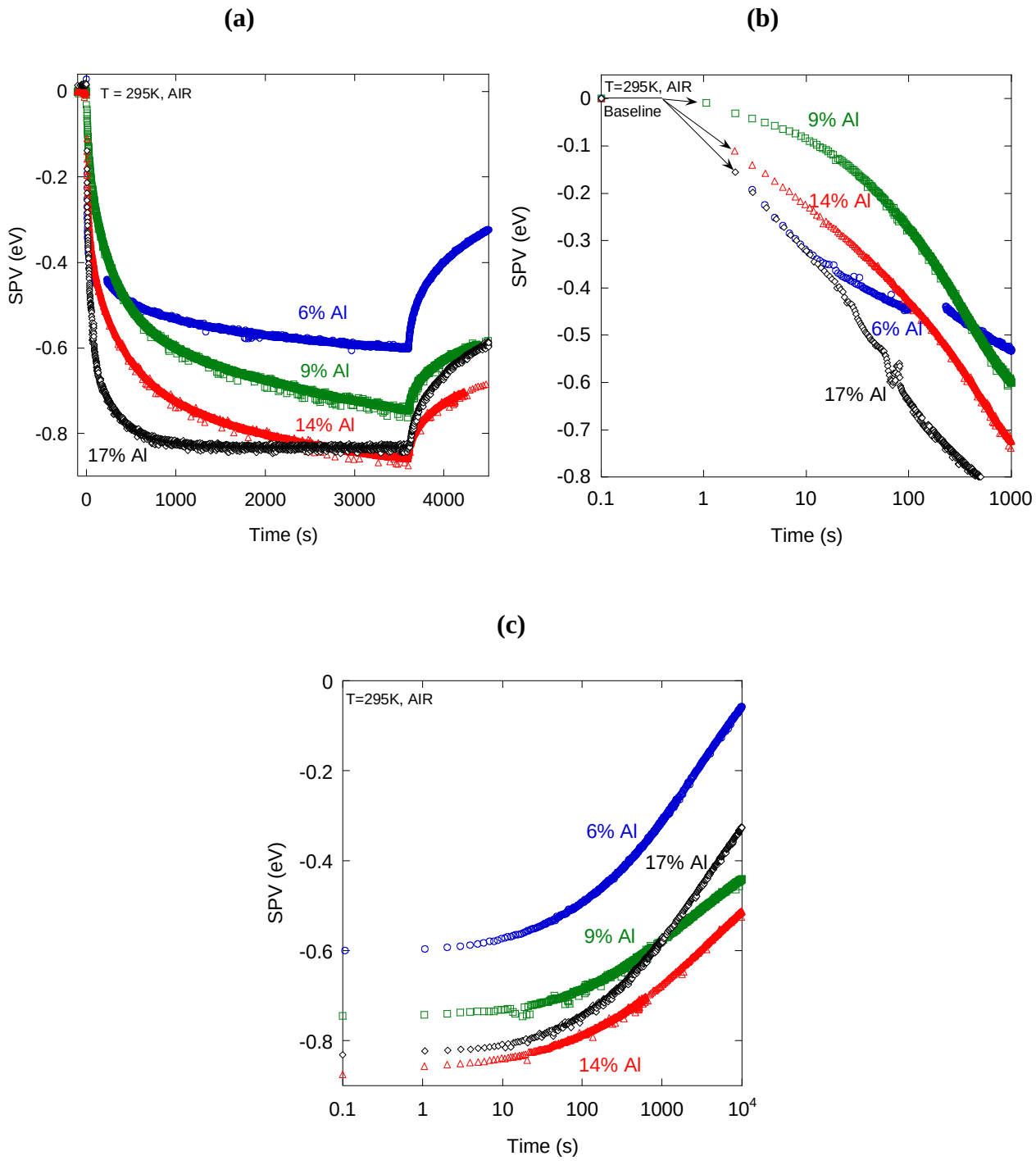

Figure 5–1. **(a)** Linearly graphed, SPV transients for various compositions of *p*-type AlGaN in air at room temperature using UV illumination (325 nm) before heat exposure from $t = 0$ to $t \approx 3600\,\text{s}$. **(b)** Initial SPV change at $t > 0$ is shown in logarithm in time scale. **(c)** Restoration after switching off the light is logarithmically graphed.

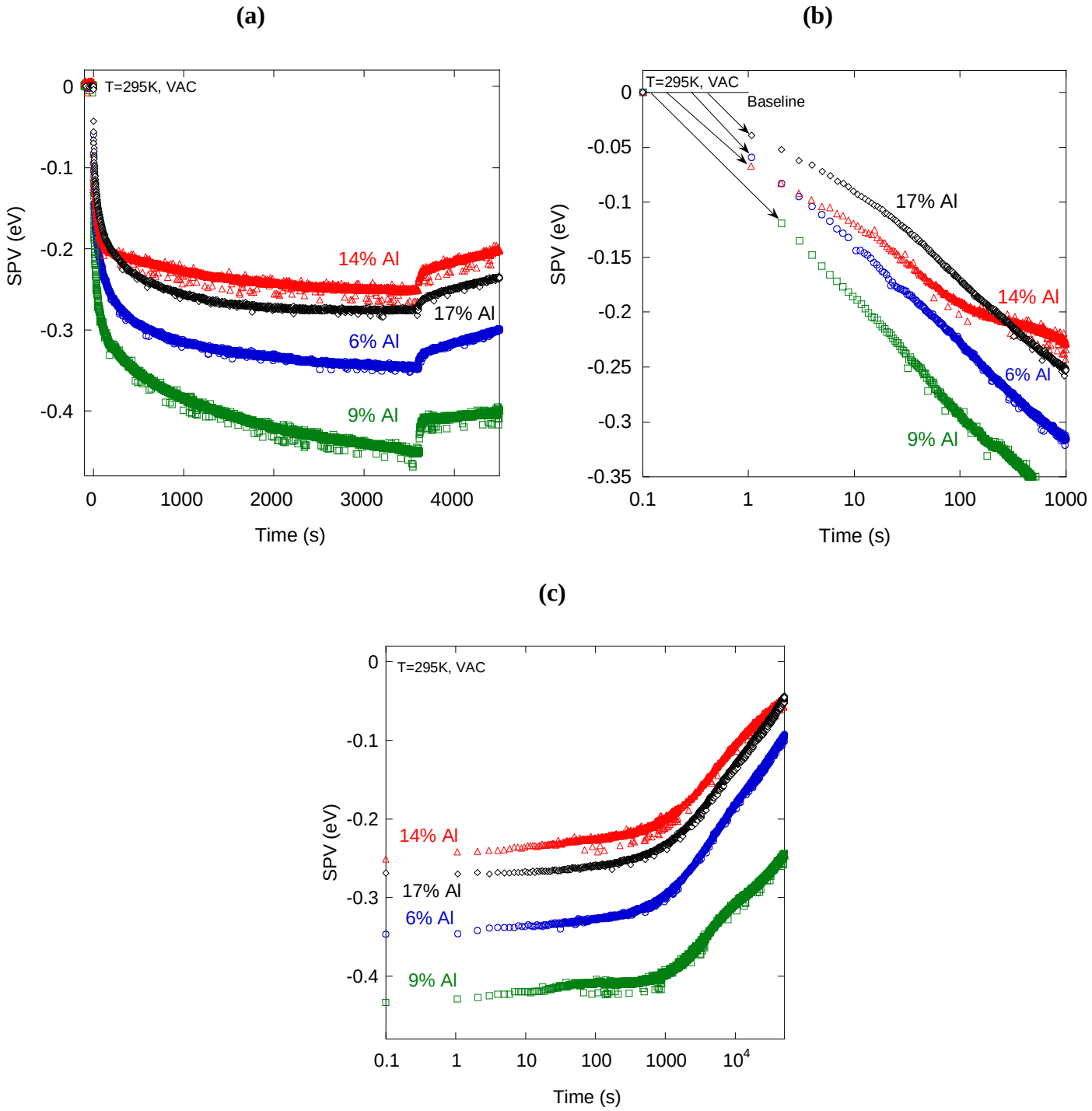

Figure 5–2. (a) Linearly graphed, SPV transients for various compositions of *p*-type AlGaN in vacuum at room temperature using UV illumination (325 nm). **(b)** Initial logarithmically graphed, SPV measurements of various compositions of *p*-type AlGaN in air at room temperature using UV illumination (325 nm). **(c)** The SPV restoration logarithmically graphed, for various compositions of *p*-type AlGaN in air at room temperature.

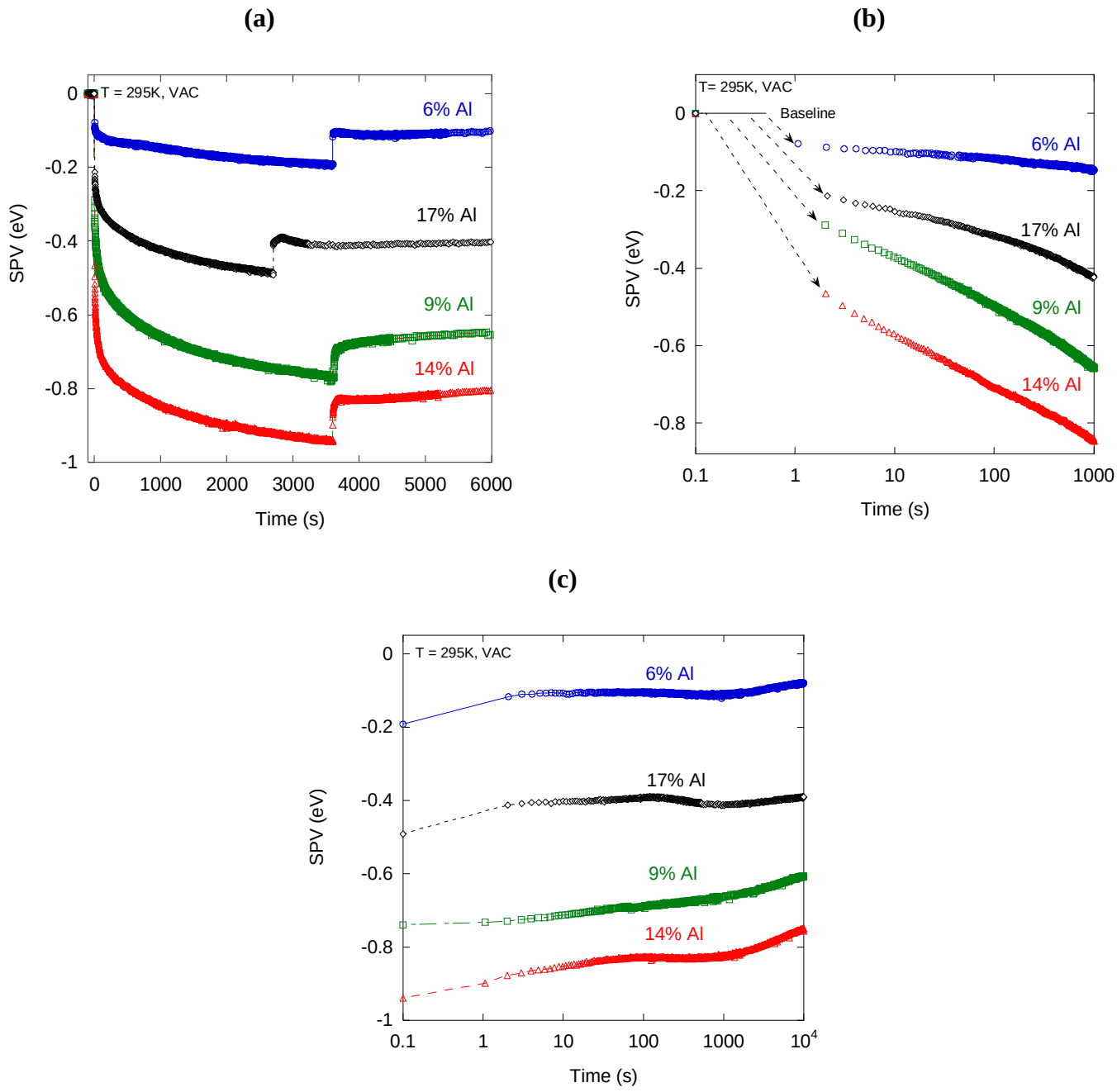

Figure 5–3. (a) Linearly graphed, SPV transients for various compositions of *p*-type AlGaN in vacuum at room temperature after preheating 500K and 600K for 1-12 hours. **(b)** Initial logarithmically graphed SPV. Horizontal bars neat the left vertical axis indicate SPV just right before turning on the laser light. **(c)** Logarithmically graphed, SPV restoration for various compositions of *p*-type AlGaN in vacuum at room temperature after heat exposure at 500K and 600K. Horizontal bars near the left vertical axis indicate SPV just before turning off the laser light.

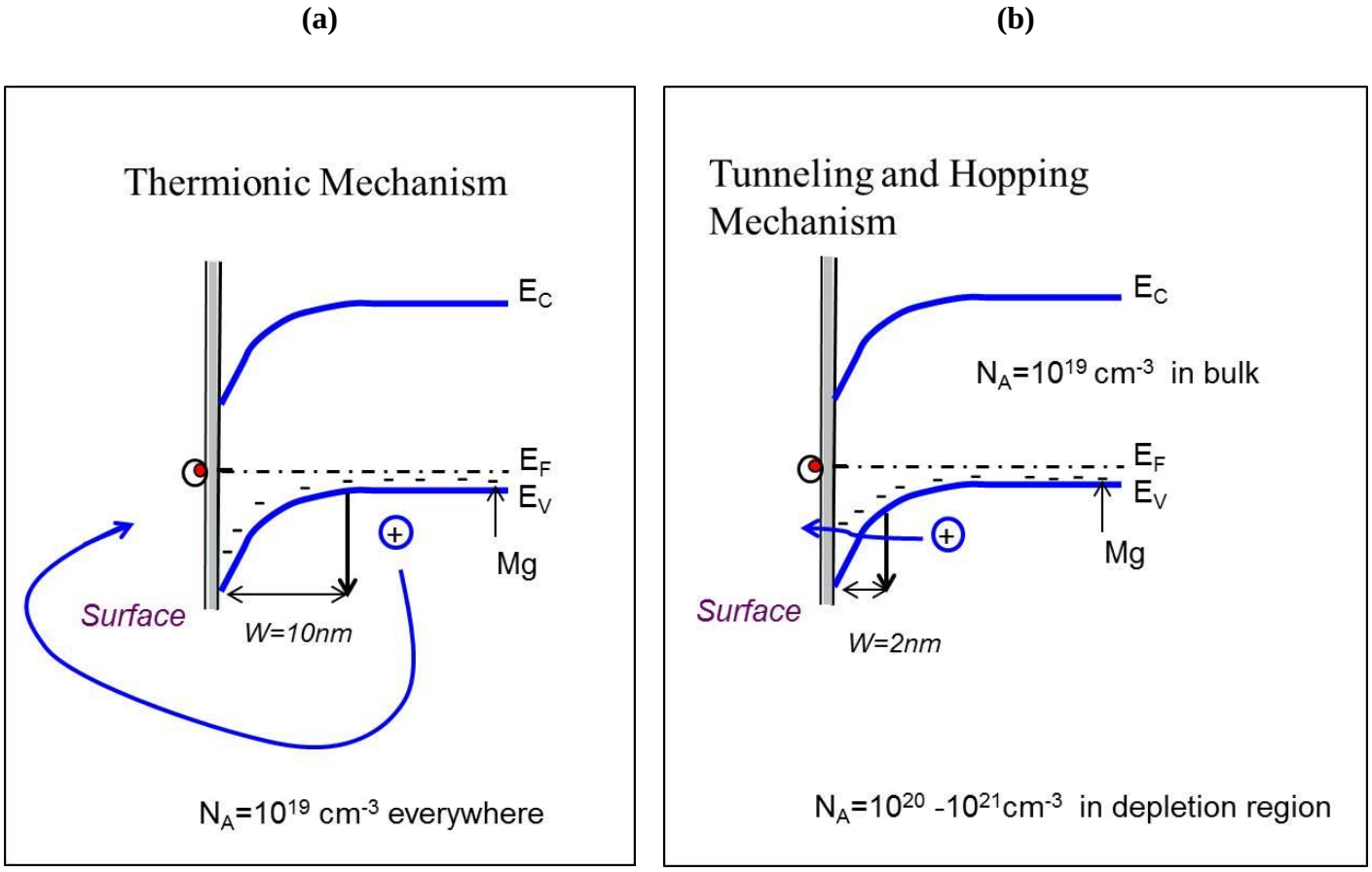

Figure 5–4. Changes in the near-surface band bending due to defect segregation. **(a)** Band bending for *p*-type AlGaN with $N_A = 10^{19}$ cm^{-3} for which the depletion region $W = 10$ nm. **(b)** With $N_A = 10^{20} – 10^{21}$ cm^{-3} in the depletion region the width becomes narrow (~2 nm). This narrow depletion region allows tunneling through the barrier, as well as hopping of holes via defect states in the depletion region to the surface.

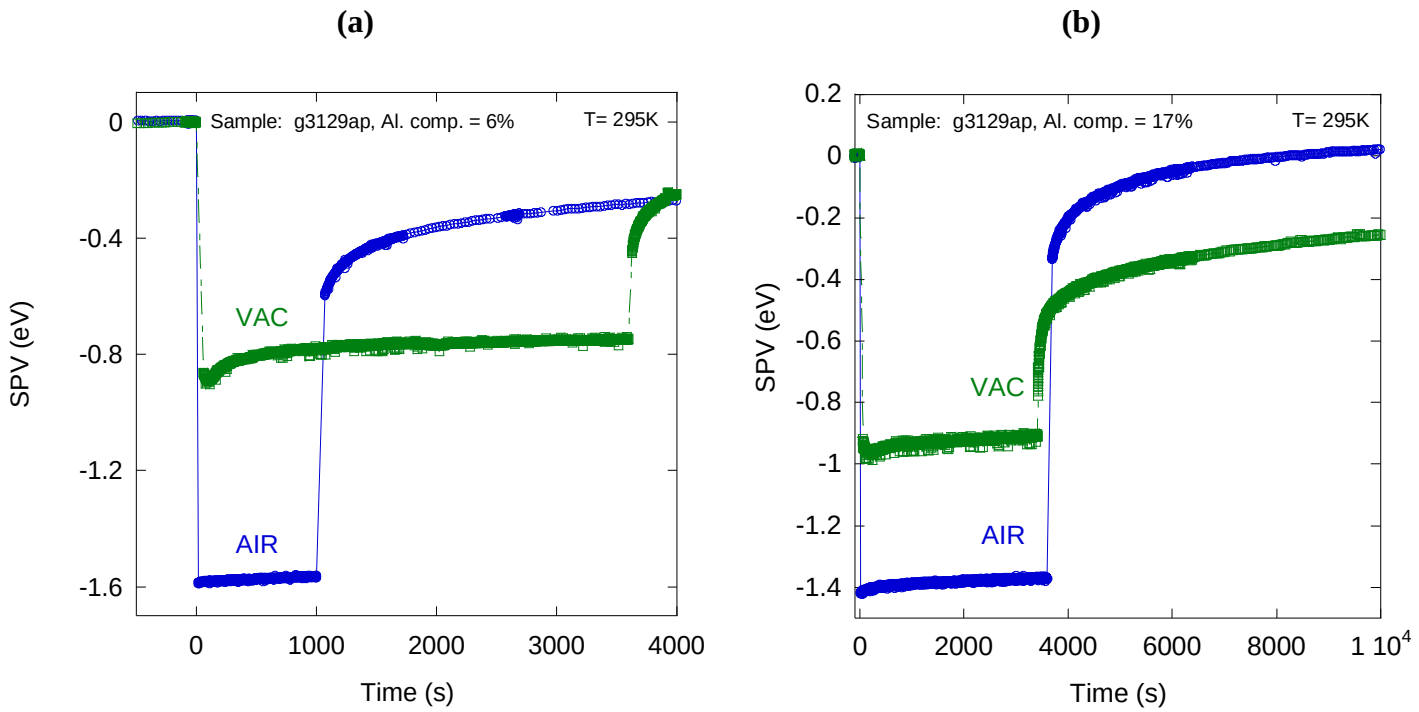

Figure 5–5. SPV transients in air and vacuum for *p*-type AlGaN sample with 6% Al and 17% Al at room temperature using UV illumination (325 nm). These measurements were taken after 40 nm was removed from the top layer by dry etching. **(a)** 6% Al was exposed to UV from $t = 0$ to $t \approx 1000$ s in air and $t \approx 3600$ s in vacuum. **(b)** 17% Al was exposed to UV from $t = 0$ to $t \approx 3600$ s in both environments.

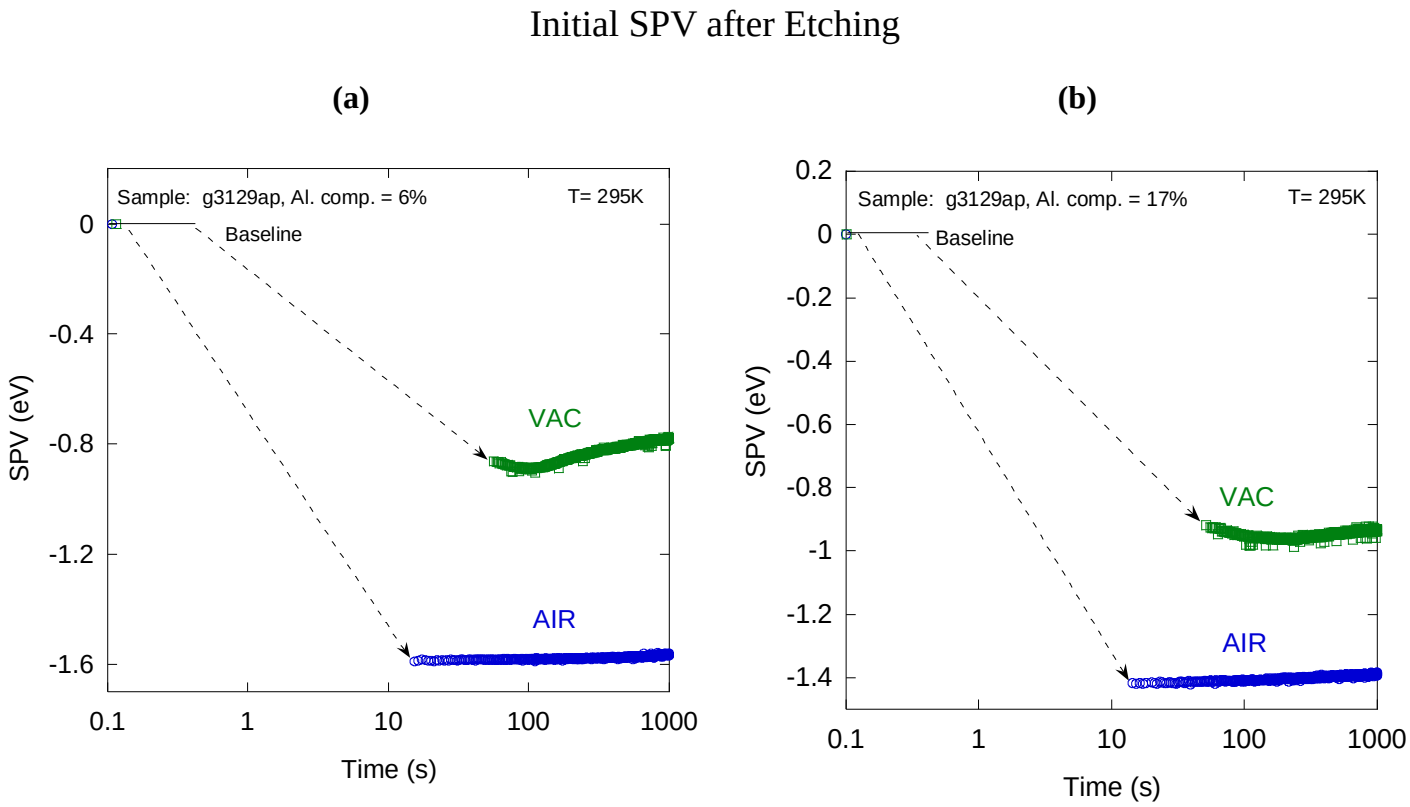

Figure 5–6. Initial SPV transients in logarithmic scale after UV illumination on at $t = 0$ in air and vacuum and at room temperature. These measurements were taken after 40 nm were removed from the top layer by dry etching. Horizontal bars near the left vertical axis indicate SPV just before turning on the laser light. **(a)** AlGaN sample with 6% of Al and **(b)** 17% of Al.

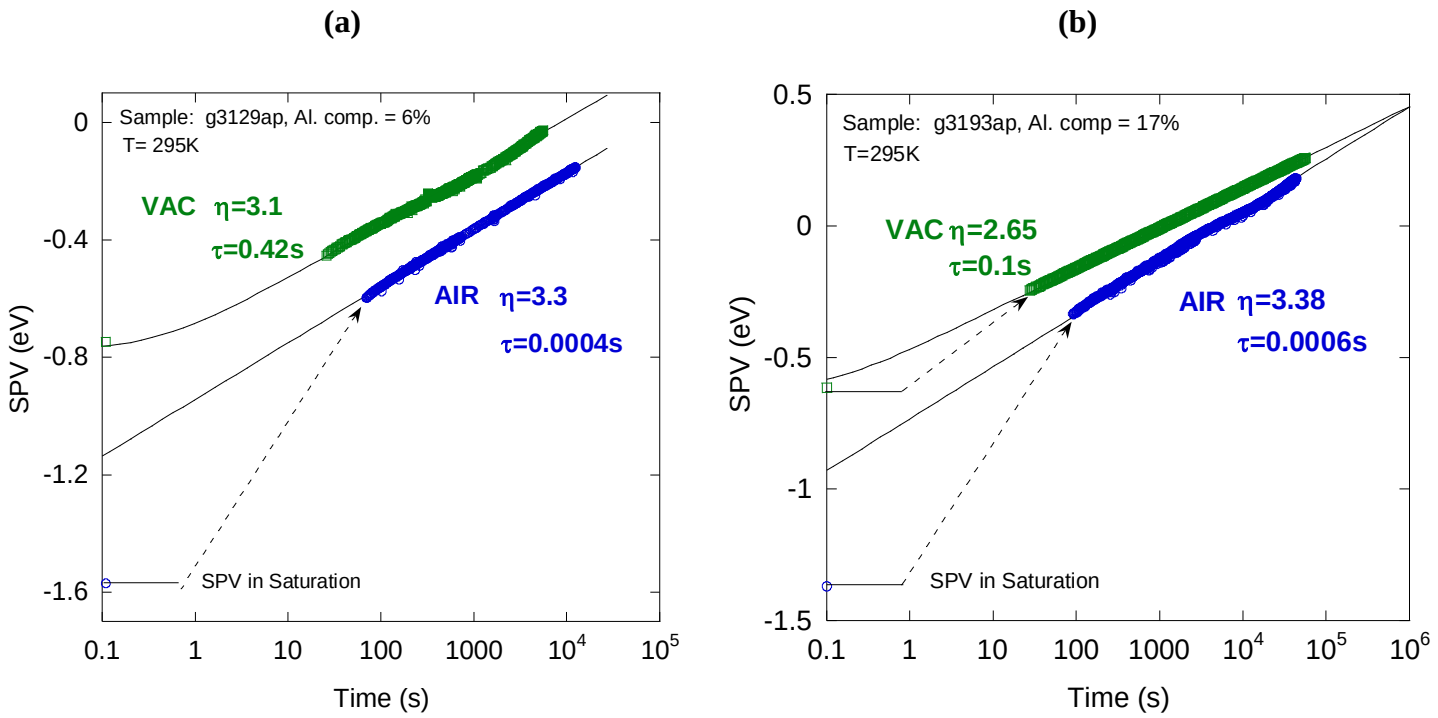

Figure 5–7. Logarithmically graphed, restoration of SPV after UV light is off at the time equal to zero. **(a)** AlGaN sample with 6% Al and **(b)** AlGaN sample with 17% of Al. Various ambients (air and vacuum) and at room temperature (295 K). These measurements were taken after 40 nm were removed from the top layer by dry etching. The solid lines show the fit using **Eq. (4-1)** of the thermionic model. In air and vacuum, the fit parameters are: (**a**) y_0 = -1.58 and -0.78 eV; η = 3.3 and 3.1, τ = 4×10^{-4} and 4.2×10^{-1} s; (b) y_0 = -1.45 and -0.52 eV; η = 3.38 and 2.65, τ = 6×10^{-4} and 1×10^{-1} s.

SPV Intensity Dependence

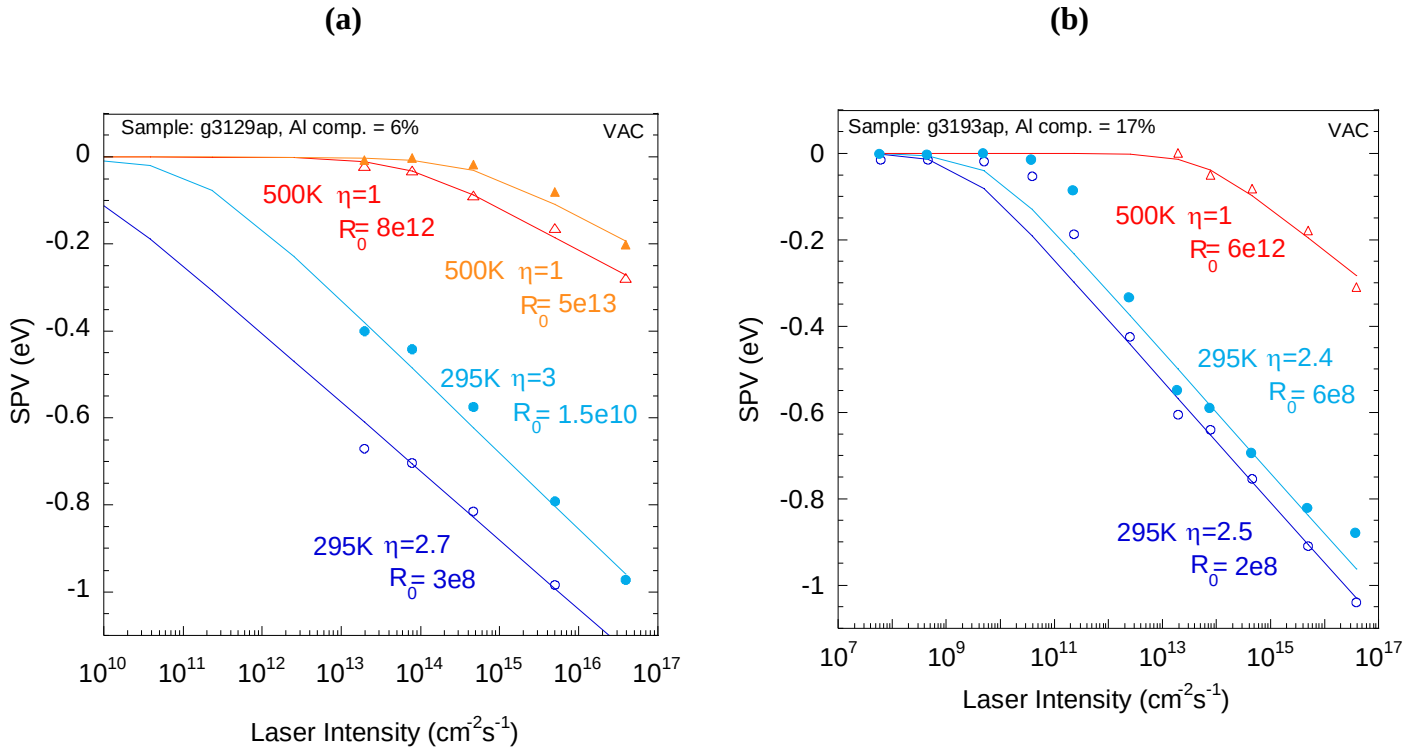

Figure 5–8. Dependence of SPV on the UV illuminations (325 nm) light intensity for AlGaN samples with 6% Al **(a)** and 17% **(b)** in vacuum at T = 295 K and T = 500 K. These measurements were taken after 40 nm were removed from the top layer by etching. The thermionic model was used to calculate the band bending in dark conditions. Solid lines are fits using **Eq. (4-2)** with the following parameters η = 2.7 and $R_0 = 3\times10^8$ for the first measurement at 295 K, η=3 and $R_0 = 1.5\times10^{10}$ for the second measurement at 295 K, η = 1 and $R_0 = 8\times10^1$ for the first measurement at 500 K, and η = 1 and $R_0 = 8\times10^{13}$ for second measurement at 500 K for the sample with 6% Al. For the sample with 6% band bending at 295 K is -2.3 eV and at 500 K is -0.8 eV. For the sample with17% Al, the following parameters are used: η = 2.5 and $R_0 = 2\times10^8$ for the first measurement at 295 K η = 2.5 and $R_0 = 6\times10^8$ for the second measurement at 295 K, and η = 1 and $R_0 = 6\times10^{12}$ for the measurement at 500 K. For the sample with 17% band bending at 295 K is -2.1 eV and at 500 K is -0.9 eV.

Conclusions

This thesis has discussed the SPV transients for *p*-type AlGaN with Al compositions between 6 and 17% obtained at different temperatures and ambients through Kelvin probe measurements. At high temperatures (500K), we were able to determine the band bending in *p*-type AlGaN, at least for the two extreme compositions of AlGaN. The downward band bending is about -1 eV for samples with composition of 6% and 17% of Al. To the best of our knowledge, this is the first report on band bending in *p*-type AlGaN.

Overall, the samples as-received showed slow transients could not be used to determine the band bending. Moreover, the SPV transients showed drastically different behavior from expected behavior as predicted by thermionic model behavior and the SPV previously observed for *p*-type GaN. We proposed that these unusual SPV transients are caused by a highly defective near-surface region, most probably created by defect segregation to the surface. Only after the defective layer has been removed by the dry etching, could fast SPV transients be observed and the thermionic model could be applied. The fit of the experimental data for the etched AlGaN samples allowed us to find the value of the band banding in AlGaN. The value at 500K (-1 eV) has been determined reliably, since the fitting parameters agreed with the expectations of the thermionic model. The value at room temperature (about -2 eV) is less accurate and less reliable since the ideality factor used in the fit is far from the factor in the thermionic model.

Appendix

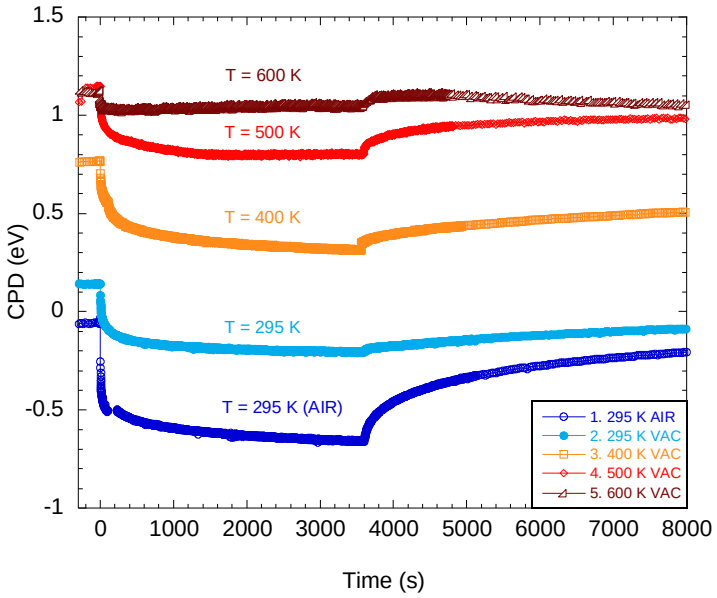

Figure A–1. SPV measurements of *p*-type AlGaN Sample with 6% Al is measurements in air and vacuum, and various temperature exposed for 1 hr of full UV (325nm) intensity.

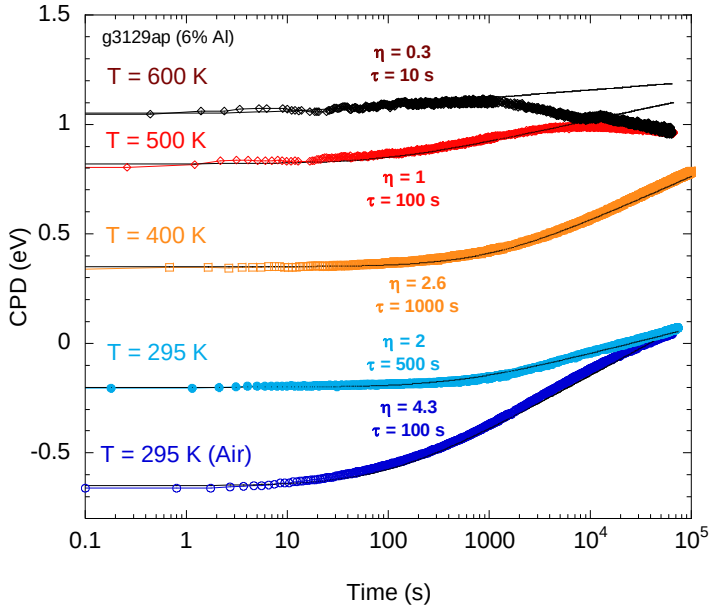

Figure A–2. Restoration SPV measurements of *p*-type AlGaN Sample with 6% Al is measurements in air and vacuum, and various temperature exposed for 1 hr of full UV (325nm) intensity with thermionic fits.

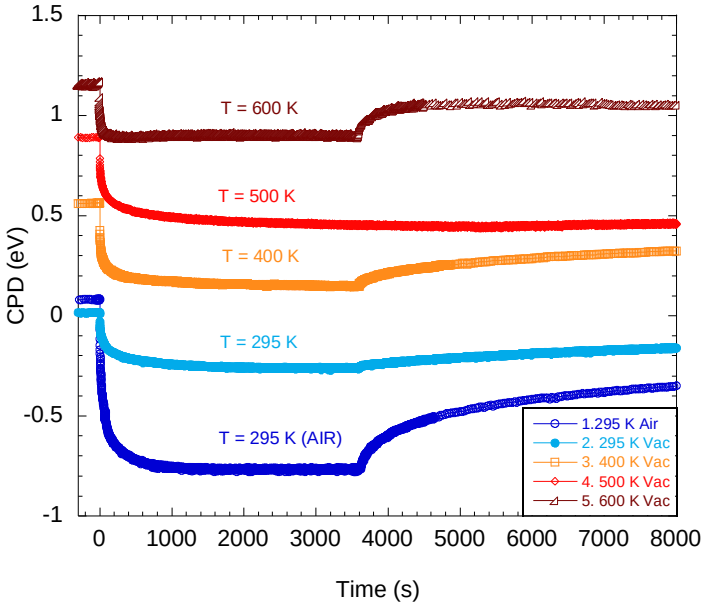

Figure A–3. SPV measurements of *p*-type AlGaN Sample with 17% Al is measurements in air and vacuum, and various temperature exposed for 1 hr of full UV (325nm) intensity.

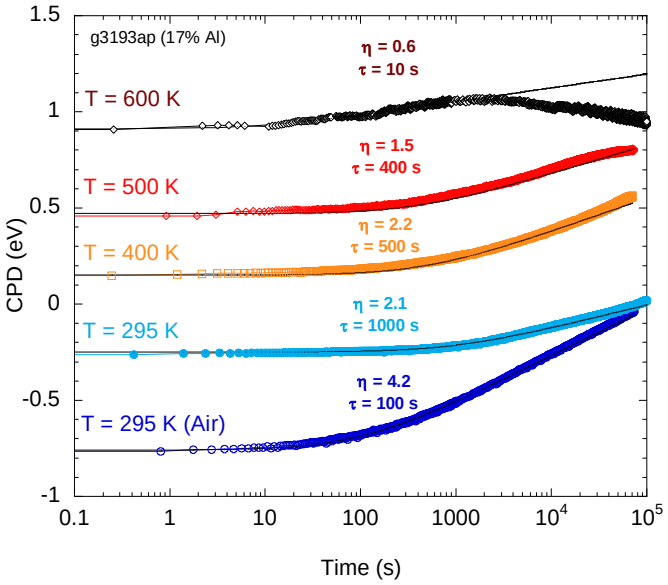

Figure A–4. Restoration SPV measurements of *p*-type AlGaN Sample with 6% Al is measug3129ap in air and vacuum, and various temperature exposed for 1 hr of full UV (325nm) intensity with thermionic fits.

References

[1] "Energy Efficiency & Costs." *Energy Efficiency and Costs*. OSRAM, n.d.

[2] "Gallium Nitride." *Gallium Nitride- Learn Chemistry*. Royal Society of Chemistry, n.d.

[3] "Global Gallium Nitride (GaN) Power Semiconductors Market worth $1.75 Billion by 2022." *Swissmetal Inc*. What's New in Business, 4 Jan. 2014.

[4] N.W. Ashcroft, N.D. Mermin. 1976. Solid State Physics. Belmont (CA): Brooks/Cole.

[5] Yang, Yibin, et. al. *Journal of Crystal Growth* **376** (2013): 23-27 (2013).

[6] H. Angerer, et. Al, *Apl. Phys. Let*. **71,** 1504 (1997)

[7] M. A. Reshchikov, M. Foussekis, and A.A. Baski. *J. Appl. Phys*. **107**, 113535 (2010)

[8] M. Foussekis, J.D. McNamara, A. A. Baski, and M.A. Reshchikov. *Appl. Phys. Let*. **101**. 082104 (2012).

[9] "Super Bright White 5mm LED." *Adafruit Industries*. N.p., n.d.

[10] Tinjum, Aaron. "The Scientists Who Invented Blue LEDs Just Won the Nobel Prize. Here's Why Their Work Matters." N.p., n.d.

[11] Taniyasu, Yoshitaka, and Makoto Kasu. "Improved Emission Efficiency of 210-nm Deep-ultraviolet Aluminum Nitride Light-emitting Diode." NTT Technical Review

[12] Image of Quantum Well for blue LED. Nichia, n.d.

[13] Image of Quantum Well with AlGaN and InGaN. N.p., n.d.

[14] Feng Yun, Michael A. Reshchikov, Lei He, Thomas King, Hadis Morkoç, Steve W. Novak, and Luncun Wei. *J. Appl. Phys*. **92,** 4837 (2002)

[15] O. Katz, B Meyler, U. Tisch, J Salzman. Phys. Stat. sol. (a) 188, No.2 789-792 (2001)

[16] S. R. Lee, A. F. Wright, M. H. Crawford, G. A. Petersen, J. Han, and R. M. Biefeld *Appl. Phys. Let*. 74, 3344 (1999).

[17] McCallister Technical Services, Kelvin probe user manual, (1997-2007)

[18] M. Foussekis, A.A. Baski, and M.A. Reshchikov. Appl. Phys. Let. **94**, 162116 (2009).

[19] B. I. Shklovskii, *Soviet Phys. JETP*. **34** (5), 1084 (1971).

[20] M. R. A. Shegelski and R. Barrier, *Phys.Rev. B.* **36** (14), 7549 (1987).

[21] B. I. Shklovskii and A. L. Efros, *Electronic Properties of Doped Semiconductors* (Springer-Verlag, Berlin), pp. 82 – 88. (1984).